Laser and Particle Beams (2009), *27*, 85–90. Printed in the USA.

doi:10.1017/S0263034609000123

Surface modifications of Ti6Al4V by a picosecond Nd:YAG laser

M.S. TRTICA,[1] B.B. RADAK,[1] B.M. GAKOVIC,[1] D.S. MILOVANOVIC,[1] D. BATANI,[2] AND T. DESAI[2]

[1]Departments of Physical Chemistry and Atomic Physics, VINCA Institute of Nuclear Sciences, Belgrade, Serbia
[2]Dipartimento di Fisica "G. Occhialini," Universita degli Studi di Milano Bicocca, Milano, Italy

(RECEIVED 24 July 2008; ACCEPTED 20 November 2008)

Abstract

Interaction of a Nd:YAG laser, operating at wavelengths of 1064 nm (23.6 J cm^{-2} fluence) or 532 nm (25.9 J cm^{-2} fluence), and pulse duration of 40 ps, with a titanium-based medical implant Ti6Al4V alloy was studied. Surface damage thresholds were estimated to be 0.9 J cm^{-2} and 0.25 J cm^{-2} at laser wavelengths 1064 nm and 532 nm, respectively. At both laser wavelengths, the energy absorbed was mostly converted into thermal energy, forming craters, albeit about 50 times deeper at 1064 nm than at 532 nm. Periodic surface structures (PSS) were also formed with both laser wavelengths, concentric, and radial at micrometer scale (3 μm to 15 μm period), parallel at nanometer scale (800 nm period with the 1064 nm laser, 400 nm with the 532 nm laser). In the case of the 532 nm laser, the concentric structures enlarge their period with accumulating laser pulse count. These features can help roughening of the implant surface and improve bio-compatibility.

Keywords: Biomaterials; Crater formation; Laser surface modification; Periodic surface structures; Picosecond Nd:YAG laser; Ti6Al4V

1. INTRODUCTION

Research of surface modifications of materials by laser beams, together with the investigation of basic principles of coupling between laser radiation and surface (Combis, 1991), are necessary to develop industrial and medical applications of laser beams. It is important to understand the processes involved, both at low levels and high levels of impact, ranging from texturing to ablation (Alti & Khare, 2006; Bussoli, 2007), as well as accompanying processes, and interactions with the plasma usually formed in front of the target (Abdallah *et al.*, 2007).

Surface modifications of different metals including their alloys by various types of laser are well-known almost as long as the laser itself. Numerous metals and their alloys have been investigated so far. Laser surface modification studies of titanium based alloys like WTi [0-1] or Ti6Al4V (Petrovic *et al.*, 2001) are of great interest. The Ti6Al4V alloy, which is the subject of the present paper, is extensively used for medical implants, and in aerospace industry. This alloy exhibits excellent physical, chemical, and mechanical properties such as thermodynamic stability, high melting point, good resistance to chemicals, etc. (Titanium: Bever, 1986). It shows comparable or better mechanical properties than many types of steel, e.g., ferritic martensitic steels.

The Ti6Al4V alloy is an important material in biomedicine (Long & Rack, 1998; Tian *et al.*, 2005; Trtica *et al.*, 2006; Mirhosseini *et al.*, 2007; Khosroshahi *et al.* 2007) as it shows a high level of bio-compatibility and bio-integration with the human body. It is corrosion resistant to electrolytes (such as physiological solution) and inert to the body fluids. It can be used as an orthopedic implant, dental implant, but also in implantable electronic devices, e.g., pacemaker housings, etc. Due to its fast decay of induced radioactivity, desirable mechanical characteristics, etc. it has been recognized as a candidate for structural material of fusion reactor components (Marmy *et al.*, 2000). It is praised in aero-space technology (Lakshmi *et al.*, 2002) due to its good reliability and excellent strength-to-weight ratio.

In bio-medical applications, the highest importance of this alloy is associated with its bio-integration. Implant surface, for example, must be contaminant-free, while roughness is its desirable morphological feature, as it plays a significant role in tissue integration (Mirhosseini *et al.*, 2007; Khosroshahi *et al.*, 2007; Bereznai *et al.*, 2003; Guillemot, 2004). Tissue cells especially tend to align along parallel

Address correspondence and reprint requests to M. S. Trtica, Department of Physical Chemistry, VINCA Institute of Nuclear Sciences, P.O. BOX 522, 11001 Belgrade, Serbia. E-mail: etrtica@vinca.rs

features (Vorobyev & Guo, 2007). The present work deals with laser modifications of a Ti6Al4V alloy surface.

Interest in the studies of laser beam interaction with the Ti6Al4V alloy has generally increased, especially in the last two decades. The Nd:YAG (Tian *et al.*, 2005; Trtica *et al.*, 2006; Mirhosseini *et al.*, 2007; Khosroshahi *et al.* 2007), cw CO_2 (Zelinski *et al.*, 2006), and various excimer (Bereznai *et al.*, 2003; Guillemot *et al.*, 2004) laser systems have so far been employed for these purposes. Interaction of this alloy with a Nd:YAG laser beam pulsed in the picoseconds time domain has not been reported so far, as that of the nanosecond/microsecond domain has (Mirhosseini *et al.*, 2007; Khosroshahi *et al.* 2007). In the present paper, we study the effects of a picosecond laser emitting in the near-infrared (1064 nm) and in the visible (532 nm) region on a medical grade Ti6Al4V alloy.

2. EXPERIMENT

Polycrystalline Ti6Al4V alloy samples were used. The samples were typically in the form of plates of dimensions 15 mm × 10 mm × 0.5 mm (length × width × thickness). The face side of each sample was polished, and the rear side was left as it is. The face roughness was evaluated by atomic force microscopy (AFM) to be less than 100 nm. Prior to laser irradiation, the sample was prepared using a standard procedure that includes cleaning, rinsing, etc.

Samples were irradiated by focusing the laser beam with a quartz lens of 12.0 cm focal length. During irradiation, the laser was operating in the fundamental transverse mode. The angle of incidence of the beam with respect to the sample surface was near 90°. The irradiation was carried out in air, at a pressure of 1013 mbar and standard relative humidity.

The laser was an active-passive mode-locked Nd:YAG system (Gakovic *et al.*, 2007). It includes a laser oscillator, an amplifier, and a non-linear crystal (KD*P). Pulse duration of about 40 ps is obtained using a saturable absorber dye and an acousto-optic standing wave modulator. The laser was operating in the TEM_{00} mode with a typical repetition rate of 2 Hz at wavelengths of 1064 nm or 532 nm.

The samples were characterized by various analytical techniques, before and after laser irradiation. Phase composition and crystal structure were determined by an X-ray diffractometer (XRD). Surface morphology was investigated by optical microscopy (OM), scanning electron microscopy (SEM), and atomic force microscopy (AFM). The SEM was coupled to an energy dispersive spectroscopy analyzer (EDS) for determining elemental surface compositions. Profilometry was used for specifying the geometry of the ablated area/crater.

3. RESULTS AND DISCUSSION

XRD phase composition analysis of the samples showed that the alloy consisted mainly of the hexagonal α-Ti phase

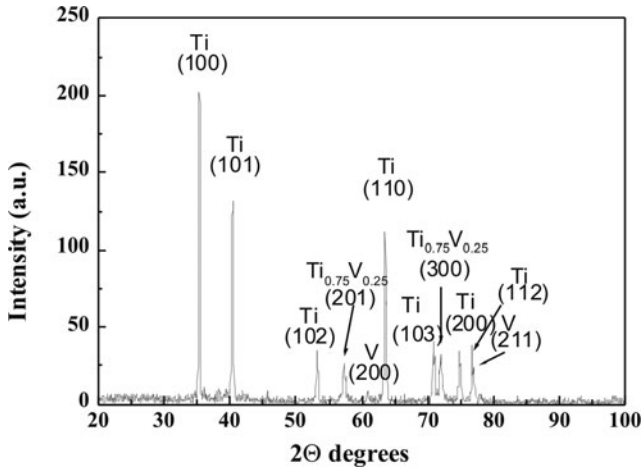

Fig. 1. XRD spectrum of non-irradiated Ti6Al4Vsurface with characteristic intensities of α-titanium labeled as Ti(100), Ti(101), and Ti(110). Ni-filtered Cu Kα radiation was used.

(Fig. 1). The most expressed peaks are attributed to hexagonal α-Ti phase like Ti(100), Ti(101), and Ti(110). Less intensive peaks of vanadium body centered cubic phase are also present. Two peaks correspond to the intermetallic compound ω-$Ti_{0.75}V_{0.25}$ with (201) and (300) orientation of planes. This is in agreement with the hexagonal structure of the α-Ti phase. The absence of aluminum peaks can be attributed to the amorphous form of the sample.

Morphological changes induced on the samples by the laser showed a dependence on beam characteristics, primarily on laser wavelength and the number of pulses accumulated.

A comparative sum-up of effects at the two laser wavelengths is given in Table 1 and a more detailed description follows below.

In both cases, craters were formed with relatively smooth centers, even after a single pulse (Fig. 2). In a separate experiment, damage threshold fluences were determined at 0.9 J cm^{-2} for the 1064 nm laser and 0.25 J cm^{-2} for the

Table 1. *A comparative sum-up of effects produced by the two laser wavelengths*

Laser at 1064 nm	Laser at 532 nm
Craters 60 μm–150 μm	Craters ≤ 2 μm
Damage threshold 0.9 J cm^{-2}	Damage threshold 0.25 J cm^{-2}
Cracks	Cracks
Hydrodynamic features	No hydrodynamic features
Oxides increased	Oxides increased
PSS, micrometer scale, period 3 μm–5 μm – radial – Concentric	PSS, micrometer scale – concentric: period 0.7 μm, enlarging to 15 μm
PSS, nanometre scale parallel waves, perpendicular to $\vec{E}$ period = 800 nm after 30 pulses	PSS, nanometer scale parallel waves, perpendicular to $\vec{E}$ period = 400 nm after 50 pulses

https://doi.org/10.1017/S0263034609000123 Published online by Cambridge University Press

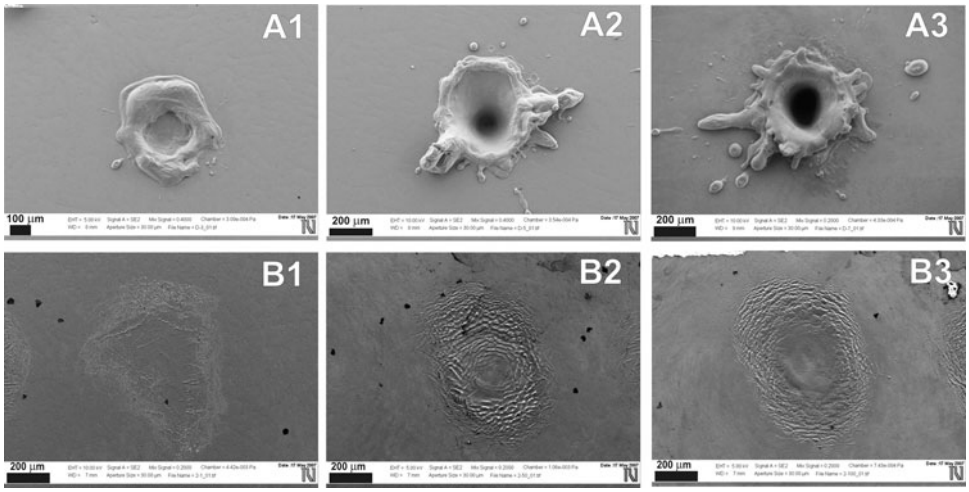

Fig. 2. SEM images of craters created by the 1064 nm and 532 nm laser beams, A-series and B-series of images, respectively. With 1064 nm, TEM_{00} mode, at 23.6 J cm^{-2}, after (A1) one pulse; (A2) five pulses; (A3) 100 pulses. With 532 nm, TEM_{00} mode, at 25.9 J cm^{-2}, after (B1) one pulse; (B2) 50 pulses; (B3) 100 pulses.

532 nm laser. For nanosecond and microsecond Nd:YAG lasers at 1064 nm, the damage thresholds have been reported to be about 0.7 J cm^{-2} (melting damage threshold, argon atmosphere) (Mirhosseini *et al.*, 2007) and 73 J cm^{-2} (etch threshold, air atmosphere) (Khosroshahi *et al.*, 2007). We have previously found that damage thresholds for this laser on a pure Ti surface are 0.9 J cm^{-2} with the 1064 nm beam, and 0.6 J cm^{-2} with the 532 nm beam (Trtica *et al.*, 2006).

Accumulation of laser pulses produced deeper craters, especially in the case of the 1064 nm laser beam, in which case depths exceeding 150 µm were obtained with 100 laser pulses.

At both wavelengths, the first and all subsequent pulses were accompanied by the appearance of spark-like plasma in front of the target.

There is a drastic difference between the depths of the craters formed by the 1064 nm and 523 nm laser beams (Fig. 3). The former is about 50 times deeper than the latter, even though similar power densities were used. This is a surprising result if one takes into account only the reflection off the sample surface, which is even higher at 1064 nm than at 532 nm. For an explanation, one has to seek other phenomena that may have prevented the 523 nm beam from inducing deeper damage in the sample.

A possible explanation is that the material ejected and the plasma that formed in front of the sample were more easily penetrated by the 1064 nm beam than by the 523 nm beam. The evaporation/ablation and plasma formation happens within a 10 ps scale (Nedialkov *et al.*, 2004), while the pulse duration is 40 ps. This means that most of the beam could have been reflected off the ejected particles and the plasma itself after a few ps into the pulse. It has also been shown that absorption of the laser energy in the plasma formed in front of the target depends strongly on the laser wavelength, and is much stronger in the visible than in the infrared region (Abdellatif Imam, 2002).

Another explanation could be based on the switching effect of VO_2 (possibly present, due to air exposure), which drastically increases the reflectance after heating up over 60°C (Barker *et al.*, 1966). However, this is hardly likely, since the effect would then be similar at both laser wavelengths, because it is not drastically wavelength dependent in this spectral region.

Since there was substantial melting and ejection of material with the 1064 nm laser, hydrodynamic features in the form of resolidified droplets were present in that case, but not in the case of the 532 nm laser, where only corrugating of the surface is visible. Cracks formed at both laser wavelengths.

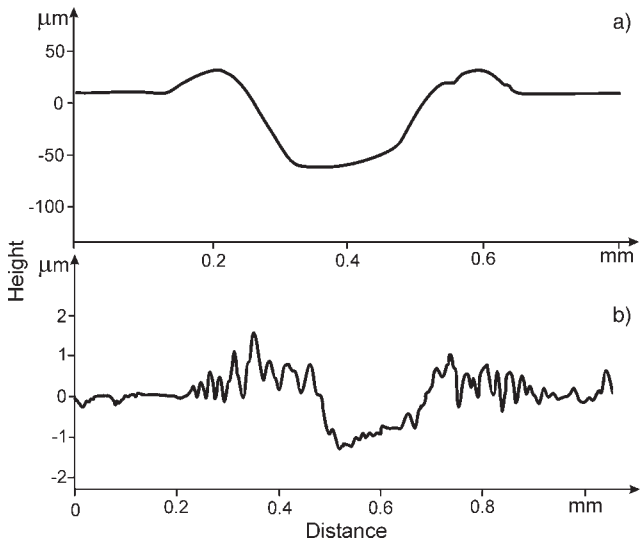

Fig. 3. Two-dimensional profilometry view of the Ti6Al4Vsurface after one pulse of the 1064 nm laser at a fluence of 23.6 J cm^{-2} (**a**), and after 50 pulses of the 532 nm laser at 25.9 J cm^{-2} (**b**).

https://doi.org/10.1017/S0263034609000123 Published online by Cambridge University Press

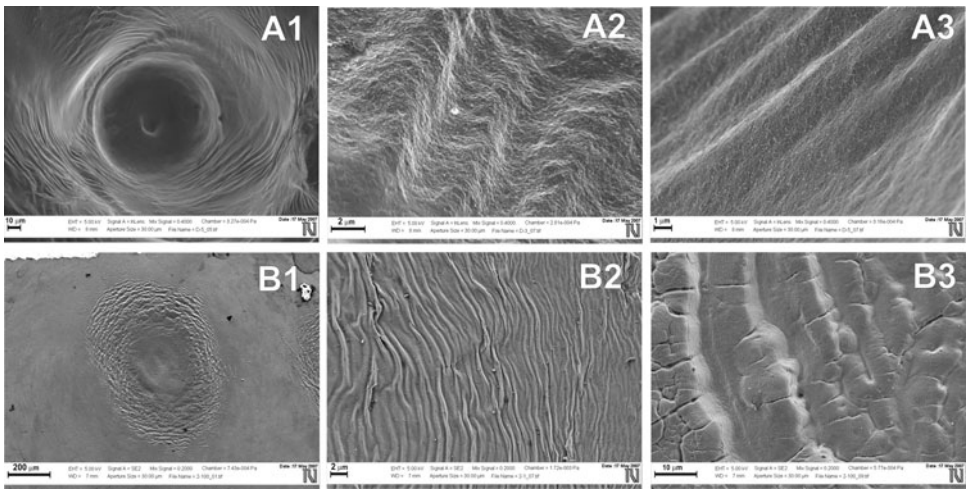

Fig. 4. SEM views of micrometer scale periodic structures formed with both laser wavelengths. With 1064 nm, TEM_{00} mode: the inside of a crater after five pulses at 23.6 J cm^{-2} (A1), and the radial (A2) and concentric periodic structures (A3) on its walls. With 532 nm, TEM_{00} mode at 25.9 J cm^{-2}: the whole crater after 100 pulses (B1), where initially concentric structures with periods below 1 μm are formed (B2), enlarging to about a 15 μm period after 100 pulses (B3).

Elemental analysis by energy dispersive spectroscopy (EDS) showed that oxygen content increased from 10%, found at the surface of the original sample, to about 14% in the centers of the damage areas at both laser wavelengths. At the rim of the damage areas, the oxygen content was found to have increased from 10% to 12% in the case of the 1064 nm laser, whereas it increased to 16% with the 532 nm laser. Oxides formed at the surface are apparently the origin of this oxygen. It is well known that titanium and its alloys, exposed to air, have a tendency to build up oxides on the surface (Sittig *et al.*, 1999), typically several nanometers thick. Oxidation is apparently increased with laser impact.

The most interesting effects observed with both laser wavelengths are the periodic surface structures (PSS). Some have periods at micrometer scale, and some at nanometer scale. The larger ones are apparently the result of melting and subsequent corrugation due to kinetic pressure. With the 1064 nm laser, both concentric and radial ripples could be observed (Fig. 4) at the walls of the craters, with periods ranging from 3 μm to 5 μm. With the 532 nm laser only concentric ripples of this kind appear. After one pulse, they are about 0.7 μm apart, but as the pulse count is increased, the ripples group together to form concentric structures with periods of about 15 μm.

The smaller periodic surface structures obtained at nanometer scale is completely different (Fig. 5). They appear as parallel ripples which are perpendicular to the laser beam electric field vector. For the 1064 nm laser, their periodicity is about 800 nm, and for the 532 nm laser, it is about 400 nm. The structures appear after accumulation of about 30 and 50 pulses, with the 1064 nm beam and 532 nm beams, respectively. These structures are formed within a diameter that is about three times wider than the full width at half maximum diameter of the laser spot. All of these facts indicate that the origin of the ripples is the interference of the incident laser beam with the so-called surface waves scattered off imperfections on the alloy surface and running along the surface (Tan & Venkatakrishnan, 2006). The periodicity of such structures (τ), is supposed to

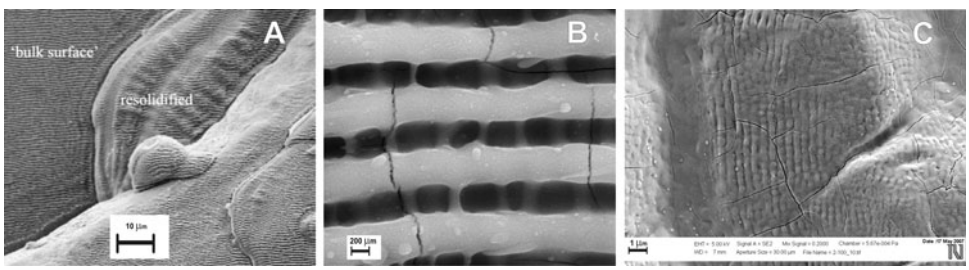

Fig. 5. SEM views of nanometer scale PSS. The same type of parallel structures formed both on the "bulk" surface and on the resolidified material: (**A**) 1064 nm laser, 100 pulses at 23.6 J cm^{-2}, produced a period of 800 nm; (**B**) detail of the structure; (**C**) 532 nm laser, 100 pulses at 25.9 J cm^{-2}, produced a period of 400 nm.

https://doi.org/10.1017/S0263034609000123 Published online by Cambridge University Press

depend directly on the laser wavelength, Eq. (1) (Tan & Venkatakrishnan, 2006):

$$\begin{aligned} \tau &\approx \frac{\lambda_{laser}}{\cos\theta_i}, && \text{for p-polarized laser beam} \\ \tau &\approx \frac{\lambda_{laser}}{1 \pm \sin\theta_i}, && \text{for s-polarized laser beam} \end{aligned} \quad (1)$$

where λ_{laser} denotes the laser wavelength, and θ_i denotes the incident angle of the beam. The beam was perpendicular in this case, thus the polarization was irrelevant with respect to the period of the ripples. The present results agree with predictions of Eq. (1), because the period of the nano-ripples decreased two times as the laser wavelength was decreased two times. It is interesting to note that these nano-structures formed on all surfaces reached by the laser beam, even on the resolidified hydrodynamic structures, and also on the apparently unaffected parts of the "bulk" surface, where the laser light was reaching the surface with much lower intensity. This can all be seen in Figure 5.

The periodicity of the structures obtained with the 532 nm laser agrees well with that obtained with the same laser, but for a completely different material, for TiN film on silicone (Gakovic *et al.*, 2007). Other authors report similar periodicities with similar laser wavelengths (Tan & Venkatakrishnan, 2006; Le Harzic *et al.*, 2005). It is important to note that none of the features of these structures indicates imprinting of a diffraction pattern originating from the optical system of the laser source, which can thus be excluded (Tarasenko *et al.*, 2002, Trtica *et al.*, 2007).

4. CONCLUSION

A study of morphological changes of a Ti6Al4V alloy surface induced by a picosecond Nd:YAG pulsed laser operating at wavelengths of 1064 nm or 532 nm with fluences of 23.6 J cm^{-2} and 25.9 J cm^{-2}, respectively, is presented. Although the fluences were similar, a significant difference was found in the induced damage. The 1064 nm laser induced almost 50 times deeper craters than the 532 nm one, most probably due to a screening effect of the ejected material and plasma, which is apparently less transparent to the 532 nm laser beam. This is why the 1064 nm laser produced hydrodynamic structures from the ejected material, and the 532 nm laser only induced corrugation of the surface.

The most interesting features produced are periodic surface structures on the micrometer and nanometer dimension scales with both laser wavelengths. In craters formed with the 1064 nm laser, both concentric and radial periodic structures appear with periods of 3 μm to 5 μm. In the case of the 532 nm laser, only concentric structures are formed, which enlarge their spacing with accumulating pulse count, from about 0.7 μm (after one pulse) to about 15 μm (after 100 pulses). At nanometer scale, parallel periodic structures are oriented perpendicular to the electric field vector, whose period depends on the laser wavelength: a period of 800 nm appears with the 1064 nm laser, and a period of 400 nm with the 532 nm laser, meaning that their origin are so-called surface waves, i.e., interference patterns of the incident laser beam with light scattered off imperfections on the surface. These structures appear in a relatively wide area, about three times wider than the full width at half maximum of the laser beam. All of these structures can be of interest in medical implant technology where the Ti6Al4V alloy is used, as a means of creating roughness that is bio-compatible with living tissues, especially parallel lines, as cells tend to align along them. For this purpose, even enhanced oxidation of the target, which was observed upon laser action helps adhesion and wear resistance.

ACKNOWLEDGMENTS

This research was sponsored by the Ministry of Science of the Republic Serbia, Contract No. 142065 and COST P-14 action. We would like to thank Dr. Peter Panjan of the Jozef Stefan Institute, Slovenia, for valuable help and support.

REFERENCES

Abdallah, J., Batani, D., Desai, T., Lucchini, G., Faenov, A., Pikuz, T., Magunov, A. & Narayanan, V. (2007). High resolution X-ray emission spectra from picosecond laser irradiated Ge targets. *Laser Part. Beams* **25**, 245–252.

Abdellatif, G. & Imam, H. (2002). A study of the laser plasma parameters at different laser wavelengths. *Spectrochimica Acta B* **57**, 1155–1165.

Alti, K. & Khare, A. (2006). Sculpted pulsed indium atomic beams via selective laser ablation of thin film. *Laser Part. Beams* **24**, 469–473.

Barker Jr., A.S., Verleur, H.W. & Guggenheim, H.J. (1966). Infrared optical properties of vanadium dioxide above and below the transition temperature. *Phys. Rev. Lett.* **17**, 1286–1289.

Bereznai, M., Pelsoczi, I., Toth, Z., Turzo, K., Radnai, M., Bor, Z. & Fazekas, A. (2003). Surface modifications induced by ns and sub-ps excimer laser pulses on titanium implant material. *Biomat.* **24**, 4197–4203.

Bever, M.B. (1986). Titanium: Alloying. In *Encyclopedia of Materials Science and Engineering*, Vol. 7, pp. 5086. Oxford: Pergamon Press.

Bussoli, M., Batani, D., Desai, T., Canova, F., Milani, M., Trtica, M., Gakovic, B. & Krousky, E. (2007). Study of laser induced ablation with focused ion beam/scanning electron microscope devices. *Laser Part. Beams* **25**, 121–125.

Combis, P., Cazalis, B., David, J., Froger, A., Louis-Jacquet, M., Meyer, B., Niérat, G., Salères, A., Sibille, G., Thiell, G. & Wagon, F. (1991). Low-fluence laser target coupling. *Laser Part. Beams* **9**, 403–420.

Gakovic, B., Trtica, M., Batani, D., Desai, T., Panjan, P. & Vasiljevic-Radovic, D. (2007). Surface modification of titanium nitride film by a picosecond Nd:YAG laser. *J. Opt. A* **9**, S76–S80.

Guillemot, F., Prima, F., Tokarev, V.N., Belin, C., Porte-Durrieu, M.C., Gloriant, T., Baquey, C. & Lazare, S. (2004).

https://doi.org/10.1017/S0263034609000123 Published online by Cambridge University Press

Single-pulse KrF laser ablation and nanopatterning in vacuum of β-titanium alloys used in biomedical application. *Appl. Phys. A* **79**, 811–813.

Khosroshahi, M.E., Mahmoodi, M. & Tavakoli, J. (2007). Characterization of Ti6Al4V implant surface treated by Nd:YAG laser and emery paper for orthopaedic applications. *Appl. Surf. Sci*. **253**, 8772–8781.

Lakshmi, S.G., Arivuoli, D. & Ganguli, B. (2002). Surface modification and characterisation of Ti–Al–V alloys. *Mat. Chem. Phys*. **76**, 187–190.

Le Harzic, R., Schuck, H., Sauer, D., Anhut, T., Riemann, I. & König, K. (2005). Sub-100 nm nanostructuring of silicon by ultrashort laser pulses. *Opt. Express* **13**, 6651–6656.

Long, M. & Rack, H.J. (1998). Titanium alloys in total joint replacement—a materials science perspective. *Biomat*. **19**, 1621–1639.

Marmy, P., Leguey, T., Belianov, I. & Victoria, M. (2000). Tensile and fatigue properties of two titanium alloys as candidate materials for fusion reactors. *J. Nucl. Mat*. **283–287**, 605–606.

Mirhosseini, N., Crouse, P.L., Schmidth, M.J.J., Li, L. & Garrod, D. (2007). Laser surface micro-texturing of Ti–6Al–4V substrates for improved cell integration. *Appl. Surf. Sci*. **253**, 7738–7743.

Nedialkov, N.N., Atanasov, P.A., Imamova, S.E., Ruf, A., Berger, P. & Dausinger, F. (2004). Dynamics of the ejected material in ultra-short laser ablation of metals. *Appl. Phys. A* **79**, 1121–1125.

Petrovic, S., Gakovic, B., Trtica, M. & Nenadovic, T. (2001). Surface modification of W-Ti coatings induced by TEA CO_2 laser beam. *Laser Part. Beams* **19**, 195–199.

Sittig, C., Textor, M., Spencer, N.D., Wieland, M. & Vallotton, P.H. (1999). Surface characterization. *J. Mat. Sci* **10**, 35–46.

Tan, B. & Venkatakrishnan, K. (2006). A femtosecond laser-induced periodical surface structure on crystalline silicon. *J. Micromech. Microengin*. **16**, 1080–1085.

Tarasenko, V.F., Fedenev, A.V., Goncharenko, I.M., Kovali, N.N., Lipatov, E.I., Orlovskii, V.M. & Shulepov, M.A. (2002). UV and IR laser interaction with metal surfaces. *SPIE Proc*. **4760**, 93–102.

Tian, Y.S., Chen, C.Z., Li, S.T. & Huo, Q.H. (2005). Research progress on laser surface modification of titanium alloys. *Appl. Surf. Sci*. **242**, 177–184.

Trtica, M., Gakovic, B., Batani, D., Desai, T., Panjan, P. & Radak, B. (2006). Surface modifications of a titanium implant by a picosecond Nd:YAG laser operating at 1064 and 532 nm. *Appl. Surf. Sci*. **253**, 2551–2556.

Trtica, M.S., Gakovic, B.M., Radak, B.B., Batani, D., Desai, T. & Bussoli, M. (2007). Periodic surface structures on crystalline silicon created by 532 nm picosecond Nd:YAG laser pulses. *Appl. Surf. Sci*. **254**, 1377–1381.

Vorobyev, A.Y. & Guo, C. (2007). Femtosecond laser structuring of titanium implants. *Appl. Surf. Sci*. **253**, 7272–7280.

Zelinski, A., Jazdzewska, M., Narozniak-Luksza, A. & Serbinski, W. (2006). Surface structure and properties of Ti6A4V alloy laser melted at cryogenic conditions. *J. Achiev. Mat. Manufact. Engin.* **18**, 423–426.

https://doi.org/10.1017/S0263034609000123 Published online by Cambridge University Press